

## Certifying the Adiabatic Preparation of Ultracold Lattice Bosons in the Vicinity of the Mott Transition

Cécile Carcy,<sup>1</sup> Gaétan Hercé,<sup>1</sup> Antoine Tenart,<sup>1</sup> Tommaso Roscilde,<sup>2</sup> and David Clément<sup>1</sup>

<sup>1</sup>Université Paris-Saclay, Institut d'Optique Graduate School, CNRS, Laboratoire Charles Fabry, 91127 Palaiseau, France

<sup>2</sup>Université de Lyon, Ens de Lyon, Université Claude Bernard and CNRS, Laboratoire de Physique, F-69342 Lyon, France



(Received 2 November 2020; accepted 8 January 2021; published 26 January 2021)

We present a joint experimental and theoretical analysis to assess the adiabatic experimental preparation of ultracold bosons in optical lattices aimed at simulating the three-dimensional Bose-Hubbard model. Thermometry of lattice gases is realized from the superfluid to the Mott regime by combining the measurement of three-dimensional momentum-space densities with *ab initio* quantum Monte Carlo (QMC) calculations of the same quantity. The measured temperatures are in agreement with isentropic lines reconstructed via QMC for the experimental parameters of interest, with a conserved entropy per particle of  $S/N = 0.8(1)k_B$ . In addition, the Fisher information associated with this thermometry method shows that the latter is most accurate in the critical regime close to the Mott transition, as confirmed in the experiment. These results prove that equilibrium states of the Bose-Hubbard model—including those in the quantum-critical regime above the Mott transition—can be adiabatically prepared in cold-atom apparatus.

DOI: [10.1103/PhysRevLett.126.045301](https://doi.org/10.1103/PhysRevLett.126.045301)

The simulation of strongly interacting quantum systems in experiments represents a most promising research effort [1], relying on the exquisite level of control acquired on different platforms—from ultracold atoms [2–4] to semiconducting [5] or superconducting [6,7] circuits. When the goal is the realization of an equilibrium state of a quantum many-body system, a paradigm common to all these platforms is that of adiabatic preparation [8,9] in the absence of an external heat bath: starting from a fiducial quantum state of an initial Hamiltonian, a continuous variation of the Hamiltonian parameters aims at transforming the state into the equilibrium state of a target Hamiltonian, at constant entropy. The successful implementation of the above paradigm is yet far from obvious, and depends on whether the state preparation is performed at (nearly) zero entropy or at finite entropy.

In platforms manipulating small ensembles ( $N \sim 10\text{--}10^3$ ) of degrees of freedom—such as trapped ions [3], atoms in optical lattices [10], Rydberg atoms [4], and quantum circuits [7]—the initial state can be prepared as the (nearly) pure ground state close to zero entropy. The conditions for its adiabatic transformation upon varying the Hamiltonian are mostly dictated by the size of the gap to the excited states [8]. The main obstacle to this *pure-state* adiabaticity is therefore offered by the vanishing of the excitation gap upon increasing the system size, e.g., at a quantum phase transition [11,12].

The situation is different for quantum simulators realizing transformations of mixed states at finite entropy. This encompasses a wealth of platforms, e.g., ranging from

ultracold atoms [2] and superconducting circuits [13] to quantum dots [5]. Extending the criteria of pure-state adiabaticity to a mixed state would suggest prohibitive conditions, as the energy gaps in the middle of the spectrum are exponentially small in the system size. Instead *mixed-state* adiabaticity does not require to follow adiabatically each pure state of the mixture, but rather to produce a state compatible with an equilibrium state of the instantaneous Hamiltonian at the same entropy. What are the conditions to guarantee such mixed-state adiabaticity? And what is the effect of quantum phase transitions (occurring in the ground state) on a finite-entropy transformation?

These are in fact formidable questions, that are being theoretically addressed only recently [14], and which are potentially hard to answer to with unbiased calculations. In experiments, keeping the entropy at a low value upon Hamiltonian transformations has always been a central preoccupation, e.g., when loading quantum gases in optical lattices [15]. But quantitative answers to the above questions are missing, mostly because a direct measure of the entropy in the experiment is hardly accessible. On the other hand, a viable route to probe the adiabatic preparation of strongly correlated quantum states at finite entropy results from the combination of experiments with *ab initio* calculations [16–21]. Indeed experimental (quasi-) adiabatic processes can be certified whenever the expected equilibrium state produced by the evolution can be efficiently simulated classically (using, e.g., quantum Monte Carlo). This program of certifying finite-entropy adiabatic processes, including the crossing of a quantum phase transition, is precisely the object of this work.

In this Letter, we study the adiabatic preparation of low-energy equilibrium states in the three-dimensional (3D) Bose-Hubbard (BH) model

$$\mathcal{H} = -J \sum_{\langle ij \rangle} (b_i^\dagger b_j + \text{H.c.}) + \sum_i \left[ \frac{U}{2} n_i (n_i - 1) + V_i n_i \right], \quad (1)$$

$b_i, b_i^\dagger$  and  $n_i = b_i^\dagger b_i$  are bosonic operators,  $\langle ij \rangle$  are nearest-neighbor pairs on the cubic lattice,  $J$  is the hopping amplitude, and  $U$  the on-site repulsive interaction energy, and  $V_i = V_x x_i^2 + V_y y_i^2 + V_z z_i^2$  is a parabolic trapping potential. At uniform integer filling  $n$  this model possesses a ground-state quantum phase transition from a superfluid (SF) phase to a Mott insulator (MI) phase upon increasing the ratio  $u = U/J$ —for  $n = 1$  the transition occurs for  $u_c = 29.34$  [22]. We implement the physics of the 3D BH model using interacting bosons of metastable helium-4 atoms ( $^4\text{He}^*$ ) loaded in a 3D optical lattice [21,23]. The lattice depth sets the value of  $u$  and provides a tool to cross the critical value  $u_c$  for the SF/MI transition [24]. Previous experiments [16] have demonstrated that slow ramps of the optical lattice produce interacting superfluid states (up to  $u \lesssim u_c$ ). Yet the adiabatic nature of the loading process, and the possible effect of the quantum phase transition on it (for  $u > u_c$ ), remains to be tested. To achieve this goal, we exploit two ingredients associated with the detection of  $^4\text{He}^*$  atoms: (i) the measurement of the 3D momentum-space density  $\rho(\mathbf{k})$  using multichannel-plate detectors [25], offering the finest level of diagnostics on the first-order phase coherence; (ii) the single-atom sensitivity that permits the study of ensembles with a moderate atom number ( $N \approx 3000$ ), with the benefit that *ab initio* quantum Monte Carlo (QMC) simulations are achievable down to low temperatures. The combination of high-resolution measurements with *ab initio* simulations allows us to certify the preparation of equilibrium states of the 3D BH model, along the trajectory defined by the above-cited atom number and by the initial entropy, which was the lowest we could achieve experimentally before ramping the optical lattice. In addition, we quantify the entropy per particle  $S/N$  in the experiment, and we find that it is conserved as  $u$  is varied (with a value  $S/N \sim 0.8k_B$ ) even when crossing the critical value  $u_c$ . This conclusion, illustrated in Fig. 1, is the main result of our work.

The experiments starts with the production of  $^4\text{He}^*$  Bose-Einstein condensates (BECs) in a crossed optical dipole trap (ODT) [26]. The BECs are then loaded into the lowest energy band of a 3D optical lattice, characterized by a lattice spacing  $d = 775$  nm and an amplitude  $V_0 = sE_r$ , where  $E_r = \hbar^2/8md^2$  is the lattice recoil energy [21,27]. In the lattice potential, the harmonic trap is isotropic with a frequency  $140(10) \times \sqrt{s}$  Hz (see Supplemental Material [28]). The BEC atom number  $N = 3.0(5) \times 10^3$  ensures a

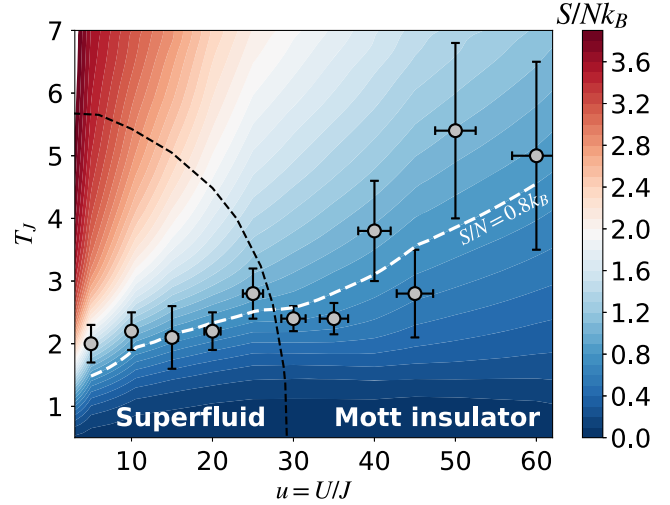


FIG. 1. Experimental reduced temperatures  $T_J = k_B T / J$  (open dots) obtained from the momentum-space-density thermometry (see text) plotted as a function of the ratio  $u = U/J$ , and compared to isentropic lines. The underlying false-color plot shows the theoretical map of the entropy per particle  $S/N k_B$  of the trapped 3D BH model, with the experimental parameters. The white dashed curve is the isentropic line at  $S/N = 0.8 k_B$ . The black dashed line represents the line of critical temperatures for the uniform 3D BH model at unit filling (from Ref. [22]).

lattice filling  $n_0$  at the trap center equal or smaller than one atom per site,  $n_0 \lesssim 1$ . To load the atoms in the 3D lattice,  $V_0$  is increased linearly at a rate of  $0.3 E_r / \text{ms}$  while the intensity of the ODT is decreased linearly to zero in 20 ms [see Fig. 2(a)]. The linear increase of  $V_0$ , which corresponds to an almost exponential increase of  $u$ , is independent of the final value of  $u$ , and the ramp is simply stopped

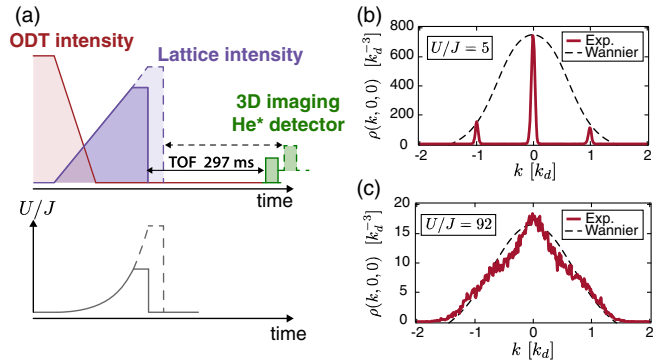


FIG. 2. (a) Time sequence for the loading of the  $^4\text{He}^*$  BECs from the optical dipole trap in the 3D optical lattice. The intensity of the 3D lattice is increased linearly with time at a rate of  $0.3 E_r \text{ ms}^{-1}$ . For two different final values of the lattice intensity, the two ramps coincide up to reaching the lowest of the two values. The linear increase of the lattice intensity corresponds to an approximately exponential increase of the ratio  $U/J$  over time. (b)–(c) 1D cut  $\rho[\mathbf{k} = (k, 0, 0)]$  along the  $\vec{u}_x$  axis through the 3D momentum-space densities measured at  $u = 5$  and  $u = 92$ .

at a later time the larger the value of  $u$ . The shape and parameters of the ramps were optimized by reducing the heating and the atom losses observed after a protocol that transfers atoms in the lattice and back to the bare ODT. The ramps used to transfer the atoms from the lattice back to the ODT are the time reversal of the loading ramps. At the final lattice amplitude  $V_0$ , we hold the atoms for 5 ms before switching off the lattice potential abruptly and letting the gas expand. We then measure the 3D distribution of individual atoms with the He\* detector after a time of flight (TOF) of 297 ms [21].

We record 3D atom distributions at various amplitudes of the lattice across the SF-MI transition, from  $u = 5$  to  $u = 92$ . For each value  $u$ , the distribution results from averaging over about  $M \sim 600$  runs of the experiment, and permits to extract the  $k$ -space density  $\rho(\mathbf{k})$ , as well as atom correlations [23,29]. Two examples of profiles  $\rho[\mathbf{k} = (k, 0, 0)]$  are shown in Figs. 2(b)–2(c). The well-contrasted peaks in Fig. 2(b) signal the extended phase coherence associated with a superfluid, in contrast with the broad distribution of the MI regime shown in Fig. 2(c). Note that the loss of coherence in the latter regime is due to the interaction, and not to heating, since ramping down  $u$  allows us to recover the interference pattern of the superfluid [23]. In contrast to previous works [16,30,31], we do not observe an incoherent background. This probably derives from the difference in the detection methods: optical probes [16,30,31] yield line-of-sight integrated 2D densities at moderate TOF durations [32,33], while the He\* detector provides us with the 3D density in the far-field regime of expansion.

The temperature  $T$  of the lattice gas cannot be extracted directly from  $\rho(\mathbf{k})$  since an analytical prediction for the trapped 3D BH model of Eq. (1) does not exist. Instead, we use a thermometry method that relies on the fact that  $\rho(\mathbf{k})$  can be obtained *ab initio* using QMC simulations. Since all the experimental parameters but the temperature are known,  $T$  is the only adjustable parameter in the comparison with QMC simulations—in particular we make use of the stochastic series expansion [34] in the canonical ensemble [35], with a fixed particle number  $N = 3000$ . More specifically,  $T$  is estimated as the temperature that minimizes the distance between the measured normalized  $k$ -space density  $\tilde{\rho}_{\text{exp}}(k) = \rho(k, 0, 0)/\rho(\mathbf{0})$  with the theoretical one  $\tilde{\rho}_{\text{QMC}}(k; T) = \rho_{\text{QMC}}(k, 0, 0; T)/\rho_{\text{QMC}}(\mathbf{0}; T)$ —focusing on the momentum cut along  $\mathbf{k} = (k, 0, 0)$ . Such a comparison relies on two assumptions that can only be verified *a posteriori*, by exhibiting a convincing agreement between the experimental and theoretical data: (i) the experiment realizes a thermal equilibrium state of the 3D BH model; (ii) the temperature of the equilibrium state is well defined in spite of the shot-to-shot fluctuations of the atom number  $N$ . The second assumption raises as well a question for the QMC calculations. In principle, the numerics should involve averaging at different atom

numbers  $N$ , which is computationally rather demanding (in particular for the entropy calculations, see below). A detailed analysis of the effect of  $N$  fluctuations (see Supplemental Material [28]) shows that such an average is not needed in practice. For the temperature and interaction regimes explored in the experiment, the quantity we use for the thermometry, namely,  $\tilde{\rho}_{\text{QMC}}(k; T)$ , shows a dependence on  $N$  that spans a smaller range in densities than that associated with the experimental uncertainty. In other words, the experiment should reproduce (within its uncertainty range) results consistent with the equilibrium behavior for the 3D BH model in the canonical ensemble. For all the lattice depths, the theoretical density  $\tilde{\rho}_{\text{QMC}}(k)$  corresponding to the optimal temperature matches well the experimental density  $\tilde{\rho}_{\text{exp}}(k)$ . This is true even in the critical regime of the Mott transition, as illustrated in Fig. 3(a) for  $u = 30$ , for which the minimum reduced chi-square corresponding to the optimal temperature is compatible with unity (see Supplemental Material [28]). This justifies *a posteriori* our working assumptions.

The results of the thermometry analysis are summarized in Fig. 1, which encompasses all the relevant regimes of the 3D BH model. In the SF regime, the reduced temperature  $T_J = k_B T/J$  is estimated with a small uncertainty

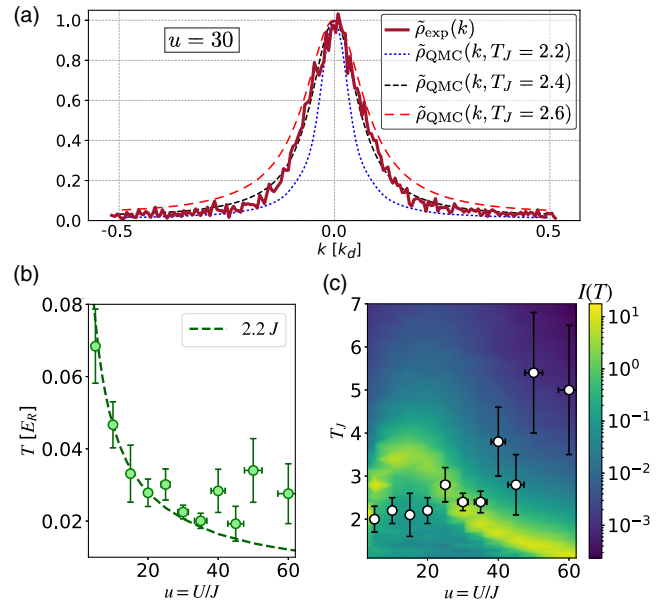


FIG. 3. (a) Plot of the momentum-space density  $\tilde{\rho}_{\text{exp}}(k)$  measured in the experiment (restricted to the first Brillouin zone) and of the theoretical one  $\tilde{\rho}_{\text{QMC}}(k; T)$  at various temperatures  $T_J$ . The comparison is shown for a ratio  $u = 30$  corresponding to the location of the quantum critical point in the ground state. (b) Measured temperature  $T$  in recoil units  $E_r$  as a function of  $u$ . The dashed line corresponds to an energy  $2.2 J$  (expressed in units of  $E_r$ ) which fits best the data in the range  $u = 5$ –20. (c) Fisher information  $I(T)$  for the temperature estimation from  $\tilde{\rho}$  obtained from the QMC data; the experimental temperatures are reproduced for reference.



( $\sim 10\%$ – $20\%$ ). In contrast, when the ground state is a MI, a significant degradation is observed. We attribute this effect to the opening of an energy gap  $\Delta$  in the excitation spectrum for the excitations localized in the center of the trap, suppressing thermal effects up to temperatures  $T \sim \Delta/k_B$ : the experimental data, due to their finite precision, become compatible with theoretical densities that span a significantly larger interval in  $T$ . Note that the small increase of  $T_J$  in the SF regime (see Fig. 1) should *not* be associated with some heating mechanism. Indeed, when  $T$  is expressed in absolute units, adiabatic cooling is observed [see Fig. 3(b)]. This descends from the fact that the isentropic gas is contained in a Bloch band whose width is proportional to  $J$  and decreases with  $s$ .

To assess the precision of the thermometry, we compute numerically the Fisher information  $I(T)$  [Fig. 3(c)] that captures the sensitivity of  $\tilde{\rho}(k)$  to variations in  $T$ , and which bounds the minimal uncertainty on the temperature obtained via the  $k$ -space thermometry [28],  $(\delta T_J)_{\min} = [I(T)M]^{-1/2}$ , with  $M$  being the number of experiment shots. We find that  $I(T)$  takes its smallest values in the Mott phase, consistent with observed loss of accuracy in the experiment. In addition, for the parameters used here,  $I(T)$  is maximal, and the temperature therefore best estimated, for  $u \sim u_c$ . The dramatic increase of  $I(T)$  close to a phase transition reflects the critical increase of the Fisher information for the whole quantum state [36]. The  $k$ -space thermometry, being optimal close to the Mott transition, is therefore ideally suited to study the adiabatic character of state preparation above the quantum critical point  $u \sim u_c$ . Importantly, the error bars on the estimated temperature exhibit a variation with  $u$  compatible with that of  $(\delta T_J)_{\min}$  set by the Fisher information. Near  $u \approx u_c$ , the uncertainty on the estimated temperature is close to the theoretical limit  $(\delta T_J)_{\min}$  [28]. This demonstrates that our implementation of the  $k$ -space thermometry with  $^4\text{He}^*$  nearly saturates its maximum allowed precision.

We now turn to discussing the entropy of the lattice gases. Along with the  $k$ -space density, the QMC simulations yield the average energy per particle  $e(T) = \langle \mathcal{H} \rangle / N$ . A high-order polynomial fit to the energy allows one to extract the specific heat  $c(T) = de(T)/dT$  and the entropy  $S(T)/N = \int_0^T d\theta c(\theta)/\theta$  [22]. The QMC calculations can access the energy and specific heat of the trapped 3D BH model down to the lowest temperatures (required to reconstruct the entropy) thanks to the moderate particle number and system sizes explored in the experiment. In view of the above assumptions, the theoretically estimated entropy should reconstruct that of the thermal equilibrium state realized in the experiment.

Figure 1 depicts the full entropy map of the trapped 3D BH model reconstructed with QMC over the temperature and interaction ranges relevant to the experiment. Besides the features of the entropy map—which we shall comment on below—the most important observation is that all the

experimental temperatures (except at  $u = 5$ ) are compatible with isentropic curves spanning the entropy range  $S/N = 0.8(1) k_B$ . The experimental data are consistent with the picture in which the lattice ramp produces a sequence of thermal equilibrium states; and in which these states are connected by transformations conserving the entropy. This represents our strongest form of certification for the adiabatic preparation of equilibrium states of the 3D BH model. In addition, the entropy of the lattice gas is compatible with the entropy  $S_0$  of the BECs before the loading in the lattice,  $S_0/N = 0.72(7) k_B$  [28]. This indicates that the transfer from the ODT to the lattice is also essentially adiabatic.

As stated previously, Fig. 1 offers an unbiased calculation of the entropy map of the trapped 3D BH model at fixed particle number. While similar calculations can be found in the literature (for the 1D and 2D BH model [37], and for the grand-canonical 3D BH model within a mean-field approximation [38]) such a map for the canonical 3D BH model has not been presented before, and it is therefore worth discussing here. For moderate entropies as those of the experiment ( $S/Nk_B \sim 0.8$ ), one distinguishes two asymptotic regimes: a SF regime ( $u \lesssim 25$ ) in which the isentropic curves show a slow growth with  $u$ ; and a MI regime (for  $u \gtrsim 35$ ) in which the isentropic curves grow more rapidly (roughly linearly with  $u$ ). A third intermediate regime separates the SF from the MI regime, in which the isentropic curves show a plateau, compatible with the experimental observations. At small  $u$ , the slow growth of the isentropic curves in the SF regime can be understood within Bogolyubov theory. In a uniform weakly interacting Bose gas, the Bogolyubov speed of sound  $c \propto \sqrt{u}$  increases with  $u$ , leading to a decrease of the density of states. The temperature dependence of the entropy is  $\sim T^3/u^2$ , implying that isentropic curves at  $S/Nk_B = s_0$  in the uniform case should grow as  $T \sim s_0^{1/3} u^{2/3}$  (within the energy range in which the dispersion relation can be approximated as  $\omega(k) = ck$ ). On the other hand, in the MI regime the entropy of a uniform system with commensurate filling goes as  $S/Nk_B \sim \exp(-\Delta/T)$ , where  $\Delta \sim u$  (for  $u \gg u_c$ ) is the MI gap, implying  $T \sim u$  along isentropic curves. Note that in the presence of a trap, the cloud wings with  $n < 1$  evolve towards a hardcore-boson regime, in which the thermodynamics becomes independent of  $u$ . The intermediate plateau regime looks somewhat unexpected on the basis of the two limiting cases, but it can be understood as resulting from a competition between the hardening of the Bogolyubov (phase) mode and the softening of the amplitude mode. The latter indeed becomes gapless at the SF/MI transition and provides a new contribution to the low-energy density of states. A detailed study of the role of the amplitude mode in the thermodynamics will be the subject of future work.

In conclusion, we have estimated the temperature of lattice gases realizing the 3D Bose-Hubbard model from a

systematic comparison between the measured momentum-space densities and large-scale unbiased quantum Monte Carlo results. In all the relevant regimes of the phase diagram, we find temperatures consistent with the preparation of equilibrium states at constant entropy  $S/N = 0.8(1)k_B$ . Our results thus indicate that the adiabatic preparation of *finite-entropy* states in quantum simulators is a rather robust property, as the adiabatic nature of the loading process is unaffected by the gapless nature of the excitation spectrum in the superfluid regime, and by the presence of the superfluid–Mott-insulator quantum critical point. This stands in contrast with systematic deviations from adiabaticity (e.g., following the Kibble-Zurek scenario) [11,12], which are expected when working at zero entropy. Our findings suggest that ultracold bosons at lower entropies than those achieved here (see, e.g., Ref. [39]), combined with flat trapping potentials, can be adiabatically prepared in the quantum-critical regime of the superfluid–Mott-insulating transition [40], which still remains largely unexplored using ultracold atoms. Moreover our work suggests that the adiabatic preparation of finite-entropy states can be a robust protocol in fermionic ultracold gases [10,19] as well as in all quantum-simulation platforms [1,7,12] investigating equilibrium phase diagrams in the vicinity of quantum critical points.

We thank H. Cayla and M. Mancini for early contributions on the experiment, and A. Browaeys, M. Cheneau, and A. Dureau for a critical reading of the manuscript. We acknowledge fruitful discussions with A. Rançon and the members of the Quantum Gas group. All the numerical simulations were performed on the PSMN facilities at the ENS of Lyon. We acknowledge financial support from the LabEx PALM (Grant No. ANR-10-LABX-0039), the Région Ile-de-France in the framework of the DIM SIRTEQ, the “Fondation d’entreprise iXcore pour la Recherche,” the Agence Nationale pour la Recherche (Grant No. ANR-17-CE30-0020-01). D. C. acknowledges support from the Institut Universitaire de France.

- 
- [1] I. M. Georgescu, S. Ashhab, and F. Nori, *Rev. Mod. Phys.* **86**, 153 (2014).
- [2] I. Bloch, J. Dalibard, and W. Zwerger, *Rev. Mod. Phys.* **80**, 885 (2008).
- [3] C. Monroe, W. C. Campbell, E. E. Edwards, R. Islam, D. Kafri, S. Korenblit, A. Lee, P. Richerme, C. Senko, and J. Smith, in *Ion Traps for Tomorrow’s Applications, Proceedings of the International School of Physics “Enrico Fermi,” Course 189*, edited by M. Knoop, I. Marzoli, and G. Morigi (IOS Press, Amsterdam, 2014).
- [4] A. Browaeys and T. Lahaye, *Nat. Phys.* **16**, 132 (2020).
- [5] T. Hensgens, T. Fujita, L. Janssen, X. Li, C. J. Van Diepen, C. Reichl, W. Wegscheider, S. Das Sarma, and L. M. K. Vandersypen, *Nature (London)* **548**, 70 (2017).
- [6] P. Roushan *et al.*, *Science* **358**, 1175 (2017).
- [7] A. D. King *et al.*, *Nature (London)* **560**, 456 (2018).
- [8] T. Albash and D. A. Lidar, *Rev. Mod. Phys.* **90**, 015002 (2018).
- [9] P. Hauke, H. G. Katzgraber, W. Lechner, H. Nishimori, and W. D. Oliver, *Rep. Prog. Phys.* **83**, 054401 (2020).
- [10] C. S. Chiu, G. Ji, A. Mazurenko, D. Greif, and M. Greiner, *Phys. Rev. Lett.* **120**, 243201 (2018).
- [11] S. Braun, M. Friesdorf, S. S. Hodgman, M. Schreiber, J. P. Ronzheimer, A. Riera, M. del Rey, I. Bloch, J. Eisert, and U. Schneider, *Proc. Natl. Acad. Sci. U.S.A.* **112**, 3641 (2015).
- [12] A. Keesling, A. Omran, H. Levine, H. Bernien, H. Pichler, S. Choi, R. Samajdar, S. Schwartz, P. Silvi, S. Sachdev, P. Zoller, M. Endres, M. Greiner, V. Vuletić, and M. D. Lukin, *Nature (London)* **568**, 207 (2019).
- [13] R. Harris *et al.*, *Science* **361**, 162 (2018).
- [14] N. Il’in, A. Aristova, and O. Lychkovskiy, [arXiv:2002.02947](https://arxiv.org/abs/2002.02947).
- [15] T. Gericke, F. Gerbier, A. Widera, S. Fölling, O. Mandel, and I. Bloch, *J. Mod. Opt.* **54**, 735 (2007).
- [16] S. Trotzky, L. Pollet, F. Gerbier, U. Schnorrberger, I. Bloch, N. V. Prokof’ev, B. Svistunov, and M. Troyer, *Nat. Phys.* **6**, 998 (2010).
- [17] R. A. Hart, P. M. Duarte, T.-L. Yang, X. Liu, T. Paiva, E. Khatami, R. T. Scalettar, N. Trivedi, D. A. Huse, and R. G. Hulet, *Nature (London)* **519**, 211 (2015).
- [18] R. Islam, R. Ma, P. M. Preiss, M. E. Tai, A. Lukin, M. Rispoli, and M. Greiner, *Nature (London)* **528**, 77 (2015).
- [19] A. Mazurenko, C. S. Chiu, G. Ji, M. F. Parsons, M. Kanász-Nagy, R. Schmidt, F. Grusdt, E. Demler, D. Greif, and M. Greiner, *Nature (London)* **545**, 462 (2017).
- [20] D. Mitra, P. Brown, E. Guardado-Sanchez, S. Kondov, T. Devakul, D. Huse, P. Schauss, and W. Bakr, *Nat. Phys.* **14**, 173 (2017).
- [21] H. Cayla, C. Carcy, Q. Bouton, R. Chang, G. Carleo, M. Mancini, and D. Clément, *Phys. Rev. A* **97**, 061609(R) (2018).
- [22] B. Capogrosso-Sansone, N. V. Prokof’ev, and B. V. Svistunov, *Phys. Rev. B* **75**, 134302 (2007).
- [23] C. Carcy, H. Cayla, A. Tenart, A. Aspect, M. Mancini, and D. Clément, *Phys. Rev. X* **9**, 041028 (2019).
- [24] M. Greiner, O. Mandel, T. Esslinger, T. W. Hänsch, and I. Bloch, *Nature (London)* **415**, 39 (2002).
- [25] F. Nogrette, D. Heurteau, R. Chang, Q. Bouton, C. I. Westbrook, R. Sellem, and D. Clément, *Rev. Sci. Instrum.* **86**, 113105 (2015).
- [26] Q. Bouton, R. Chang, A. L. Hoendervanger, F. Nogrette, A. Aspect, C. I. Westbrook, and D. Clément, *Phys. Rev. A* **91**, 061402(R) (2015).
- [27] A. Tenart, C. Carcy, H. Cayla, T. Bourdel, M. Mancini, and D. Clément, *Phys. Rev. Research* **2**, 013017 (2020).
- [28] See Supplemental Material at <http://link.aps.org/supplemental/10.1103/PhysRevLett.126.045301> for a discussion of the microscopic parameters used in the QMC calculations, the detailed chi-square analysis of the temperature estimate, the Fisher information associated to the  $k$ -space thermometry, the role of the atom number fluctuations on the thermometry method, the QMC estimate of the entropy, and the measurement of the entropy of the BECs before the loading in the lattice.

- [29] H. Cayla, S. Butera, C. Carcy, A. Tenart, G. Hercé, M. Mancini, A. Aspect, I. Carusotto, and D. Clément, *Phys. Rev. Lett.* **125**, 165301 (2020).
- [30] K. Xu, Y. Liu, D. E. Miller, J. K. Chin, W. Setiawan, and W. Ketterle, *Phys. Rev. Lett.* **96**, 180405 (2006).
- [31] D. McKay, U. Ray, S. Natu, P. Russ, D. Ceperley, and B. DeMarco, *Phys. Rev. A* **91**, 023625 (2015).
- [32] F. Gerbier, S. Trotzky, S. Fölling, U. Schnorrberger, J. D. Thompson, A. Widera, I. Bloch, L. Pollet, M. Troyer, B. Capogrosso-Sansone, N. V. Prokof'ev, and B. V. Svistunov, *Phys. Rev. Lett.* **101**, 155303 (2008).
- [33] U. Ray and D. M. Ceperley, *Phys. Rev. A* **87**, 051603(R) (2013).
- [34] O. F. Syljuåsen and A. W. Sandvik, *Phys. Rev. E* **66**, 046701 (2002).
- [35] T. Roscilde, *Phys. Rev. A* **77**, 063605 (2008).
- [36] M. Mehboudi, A. Sanpera, and L. A. Correa, *J. Phys. A* **52**, 303001 (2019).
- [37] L. Pollet, C. Kollath, K. V. Houcke, and M. Troyer, *New J. Phys.* **10**, 065001 (2008).
- [38] S. Yoshimura, S. Konabe, and T. Nikuni, *Phys. Rev. A* **78**, 015602 (2008).
- [39] B. Yang, H. Sun, C.-J. Huang, H.-Y. Wang, Y. Deng, H.-N. Dai, Z.-S. Yuan, and J.-W. Pan, *Science* **369**, 550 (2020).
- [40] S. Sachdev, *Quantum Phase Transitions* (Cambridge University Press, Cambridge, England, 2011).